Microencapsulation of Dragon Fruit Peel Extract by Freeze-Drying Using Hydrocolloids: Optimization by Hybrid Artificial Neural Network and Genetic Algorithm

G. V.S. Bhagya Raj
Tezpur University
Kshirod K. Dash (kshirod@tezu.ernet.in)
Tezpur University

Research Article

Keywords: dragon fruit, ultrasound, encapsulation, artificial neural network, genetic algorithm

Posted Date: March 11th, 2022

DOI: https://doi.org/10.21203/rs.3.rs-1432238/v1

Abstract

The freeze drying encapsulation process was used to encapsulate dragon fruit peel extract with three distinct wall materials: maltodextrin, gum arabica, and gelatin. The process was modeled using a feed forward back propagation artificial neural network with four, eleven, and four neurons in the input, hidden, and output layers. Three of the four input neurons were concentrations of wall material (g), while the fourth was ultrasonication power. The four output neurons were encapsulation efficiency, antioxidant activity, hygroscopicity, and solubility of freeze-dried encapsulation powder. The procedure was optimized using hybrid artificial neural network (ANN) and genetic algorithm (GA) approach. The optimal wall material composition for encapsulation obtained by the integrated ANN and GA was 4.461 g maltodextrin, 3.863 g gum arabic, and 3.198 g gelatin. The optimal ultrasonication power for achieving a homogenous mixture was determined to be 123 W. At the optimal condition, the predicted values for the responses encapsulation efficiency, antioxidant activity, hygroscopicity, and solubility were found to be 88.143%, 81.702%, 6.924 g/100g, and 32.841%, respectively. Under optimal conditions, the relative deviation between the predicted model and experimental outcomes was less than 2.077%. The thermal stability of the encapsulated powder followed the first order kinetic modeling. The results showed that the sample treated at pH of 7 was more thermally stable at 80°C than the sample treated at pH of 3.6. The half-life time was found to be 140 min and 103 min for the sample treated at pH of 7 and 3.6, respectively.

1. Introduction

Dragon fruit, known for its distinct look and delicate texture, belongs to the family of Cactaceae and is a vine climbing cactus of the *Hylocereus* genus (Hua et al., 2018). Dragon fruit used to be a backyard plant grown only for table consumption and medicinal uses. But now, there is a global growth of dragon fruit production from which growers are getting benefitted (Balendres & Bengoa, 2019). The pulp of dragon fruit has a high concentration of vitamin C as well as water-soluble fiber. The reddish color imparted to the peels of *Hylocereusundatus* is associated with persistent nitrogen containing pigment known as betacyanin, which are water soluble (Al-Mekhlafi et al., 2021). The peel of the fruit was a major byproduct of the dragon fruit juice processing industry and generally dumped onto the ecosystem. Recent research on dragon fruit peel was aimed at extracting polyphenols, betacyanin (G. V.S. Bhagya Raj & Dash, 2020b), and pectin (Tien et al., 2022).

The temperature during food processing and storage significantly impacts betacyanin stability since heating induces the breakdown of this pigment (Gengatharan et al., 2015; Herbach et al., 2006). In addition to these factors that degrade the stability of betacyanin were light exposure, pH, water activity, soluble metals, and enzymatic reactions (Edia Rahayuningsih et al., 2021). Degradation and low stability of betacyanin can be the major issue in use as a food colorant in the food matrix. As natural dyes' potential and drawback, some innovation is necessary to minimize natural dyes' disadvantages as food colorants (E. Rahayuningsih et al., 2019). The utilization of betacyanin in food processing can be increased by enhancing its stability, which can be accomplished by the encapsulation method. Therefore encapsulation of can be a substantial alternative approach for boosting the stability of bioactive substances.

Encapsulation is a technique in which targeted compounds are entrapped by encapsulant in order to form capsules or microcapsules at micrometer or nanometer scale and eventually released at the time of requisite (Bamidele & Emmambux, 2021). The encapsulation method was extensively applied in food processing industries to encapsulate phytochemicals such as polyphenols, micronutrients, enzymes, and antioxidants by creating protective barriers against the light, oxygen, pH, moisture, heat, shear, or other extreme conditions during processing and storage. It improves the stability of the product when transiting through the gastrointestinal tract (Dima et al., 2015). Different methods were implemented to achieve the encapsulation of phytochemicals from food materials, including wet heat processing (pasting, kneading, and co-precipitation), spray drying, spray cooling/chilling, extrusion coating, fluidized bed coating, liposome entrapment, coacervation, inclusion complexation, centrifugal suspension separation, co-crystallization, liposomes, nanoparticles, freeze-drying, emulsion and rotational suspension separation (Boger et al., 2021; Carpentier et al., 2021; Lengyel et al., 2019). Usually, the encapsulation process consists of two main steps, such as homogeneous mixing of components and drying. Ultrasound treatment can be applied for homogeneous mixing, and it is an effective, non-toxic, and environmentally friendly process that shortens the drying time (Colucci et al., 2018; Yazicioglu et al., 2015).

The freeze-drying encapsulation technique was commonly utilized to entrap phytochemicals from agricultural products into another material because the core molecules are heat sensitive (Cheng et al., 2017; Yamashita et al., 2017). As mass transfer in freeze drying does not occur by evaporation but rather through freezing, sublimation, and desorption for dehydrating the material, the powder is formed when the frozen feed emulsion is sublimated. (Ozkan et al., 2019). The freeze drying technique was successfully implemented to microencapsulate bioactive compounds from fruits and vegetables with different wall materials such as encapsulation of betanin (a natural dye of red beets) in a combination of maltodextrin and xanthan gum, bioactive compounds of Malpighia emarginata DC fruit pulp extracts using gum arabica and maltodextrin (Rezende et al., 2018), Anthocyanin of purple Roselle with maltodextrin as carrier agent (Nafiunisa et al., 2017), betalain extract from Cactus pear fruit by starch and maltodextrin as wall materials (Morales et al., 2021), anthocyanins from pomegranate peel using maltodextrin and calcium chloride (Azarpazhooh et al., 2019), red beet root extract using carrier agents as maltodextrin and whey protein isolate (Faridnia et al., 2020) and curcumin with various wall materials (Guo et al., 2020).

Maltodextrin is a polysaccharide that is commonly used as a carrier agent for microencapsulation due to its high solubility in water (Galves et al., 2021). The solutions formed from maltodextrin are colorless, with low viscosity and sugar content, and are inexpensive (Akhavan Mahdavi et al., 2016; Robert et al., 2010). Gum Arabic is a natural polysaccharide and exudate gum of acacia that is widely utilized as an efficient wall material in various food applications (Carpentier et al., 2022). Gum Arabic is preferred as a carrier agent due to emulsion formation and excellent volatile retention ability (Rajabi et al., 2015). Gelatin has good biocompatibility and biodegradability and is a polypeptide with high molecular weight derived by regulated hydrolysis of collagen from bones and skin (Elzoghby, 2013; Nezhadi et al., 2009). It has the ability to form a film and a gel with excellent mechanical properties that also serve as barriers to oxygen, carbon dioxide, and volatile compounds (Tongnuanchan et al., 2012). Xanthan gum is a colorless, tasteless, odorless, and smooth texture. Xanthan gum has low viscosity at high shear rates and high viscosity at low shear rates. It has stability against heat, acid, and alkali conditions and is a clear weak gel-like liquid that can be used in a variety of industrial applications (Jo et al., 2018). Use of one carrier agent or wall material for encapsulation is not preferable

as it does not maintain all necessary properties to retain the core material. As a result, a wall material comprising two or more carrier agent mixtures could be employed to increase the encapsulation characteristics of the compound of interest. This could be accomplished by combining carbohydrates with proteins and polysaccharides in various proportions.

The artificial neural network is considered a powerful tool to develop mathematical models with higher accuracy and flexibility for modeling processes and predicting responses (G. V.S. Bhagya Raj & Dash, 2020a; Huang et al., 2017). In many of the ANN modeled food processing methods, genetic algorithm (GA) was used for optimizing the process parameters such as microwave puffing (K. K. Dash & Das, 2021), ultrasound-assisted extraction (G. V.S. Bhagya Raj & Dash, 2020b), convective drying (Chasiotis et al., 2020), spray drying (Przybył et al., 2018), and microwave vacuum drying (Khawas et al., 2016). Many researchers integrated ANN with GA for modeling and optimizing the encapsulation process, such as phenolic extracts from different agricultural produces (Espinosa-Sandoval et al., 2019), blueberry anthocyanin extract (Tao et al., 2017), and olive pomace phenols (Aliakbarian et al., 2018). There has only been a little research on the effect of hydrocolloids and ultrasound on the encapsulation process. Based on this, the objective of this study is to encapsulate the phytochemicals of dragon fruit peel by using the freeze drying technique using three different wall materials such as maltodextrin, gum arabica, and gelatin. The influence of wall materials and ultrasonication power on encapsulation efficiency, antioxidant activity, hygroscopicity, and solubility of the encapsulated product was studied using a feed-forward back propagation neural network, and the process was optimized by using integrating ANN–GA approach.

2. Materials And Methods

2.1 Raw materials

Dragon fruits (*Hylocereus undatus*) were procured from the local markets of Tezpur, Assam, and were cleaned thoroughly to free from foreign materials. Then the dragon fruit peel was separated from the pulp of the fruit, and peels were dried in a freeze dryer (Lyolab Freeze Lab, Lyophilization Systems Inc., USA). The dried peels were ground into powder and passed through a mesh of size 0.25 mm.

2.2 Ultrasound assisted extraction

The phytochemicals from freeze-dried dragon fruit peel powder was extracted with the application of ultrasound. The extraction was carried out at 100 W of ultrasonication power, 60°C of ultrasonic temperature, 60% of ethanol concentration, 25:1 mL/g of solvent to solid ratio, and 20 min of ultrasonic treatment time (G. V.S. Bhagya Raj & Dash, 2020b). After the extraction, the extract was stored at − 18°C for further analyses.

2.3 Microencapsulation of dragon fruit peel extracts by freeze–drying

Plain maltodextrin (X_1), gum arabic (X_2), and gelatin (X_3) were used as the encapsulating agents for the freeze-drying encapsulation method. Ultrasound power (X_4) was implemented for homogenize mixing of wall material and extract. The experiments of encapsulation process of dragon fruit peel extract by freeze drying were designed using central composite design that yielded 30 experiments. The process was modeled and optimized using a combined feed forward back propagation neural network and genetic algorithm. For the experimental design, different combinations of encapsulating agents with the range from 1 to 5 g and ultrasonication power with a range from 100 to 300 W were selected as independent variables with five levels. The effect of these four independent variables on the physicochemical properties of freeze-dried encapsulated powder, i.e., encapsulation efficiency (Y_1), antioxidant activity (Y_2), hygroscopicity (Y_4) and solubility (Y_4) were studied, and these were selected as dependent variables or responses of the model.

The three selected encapsulating agents were formed into wall material compositions for freeze drying encapsulation according to the design. The mixture of the encapsulating agents was dissolved in distilled water and mixed using a magnetic stirrer at 25^{o}C to obtain 20% total solid concentration. The solution was stored at 4°C for 24 h to attain complete hydration. The ultrasonic assisted dragon fruit peel extract was progressively added to the solution comprising wall materials in a weight ratio of 1:1 (wall material: extract (w:w)). The mixture was mixed under vigorous magnetic stirring and the pH value was adjusted to 2.0. To ensure complete homogenization, samples were further sonicated at different power according to the experimental design at room temperature for 5 min. The homogenized mixture of wall agents and core was dried using a freeze drier (Lyolab Freeze Lab, Lyophilization Systems Inc., USA). The dried samples were ground into fine powder and then packed in polyethylene bags, and stored at 4°C for further analysis.

2.4 Modeling and optimization

Feedforward backpropagation ANN was applied for modeling of the encapsulation process by freeze-drying with one layer in input, hidden, and output layer, shown in Fig. 1. The freeze-drying encapsulation was modelled using an artificial neural network with four input neurons that are independent variables and four output neurons or responses. The experimental data sets were split into three groups, each with a proportion of 70, 15, and 15 for training, testing and validation of the model, respectively. The neurons in the hidden layer were varied from 2 to 15, and the number of neurons in the hidden layer of the ANN model was selected based on the lower MSE value of ANN training. Levenberg–Marquardt algorithm was used for the training of the ANN model. The log sigmoid function whose range was − 1 to + 1 for input neurons and 0 to + 1 for output neurons was used as activation function between the input and hidden layer and hidden and output layer. The independent neurons were the amount of maltodextrin, gum arabica, gelatin, and ultrasonication power. The real values of input neurons were designated as X_1, X_2, X_3 and X_4 respectively and their coded values as x_1, x_2, x_3 and x_4 respectively. Similarly, the real values of dependent variables encapsulation efficiency, antioxidant activity, hygroscopicity, and solubility of the freeze-dried encapsulated product was assigned as Y_1, Y_2, Y_3 and Y_4 respectively and their respective coded values as y_1, y_2, y_3 and y_4 respectively.

The weights between input and hidden layer and the weights between hidden and output layer was assigned as w_{hi} and w_{oh} respectively. The bias matrix at hidden was designated as b_{h1} and at output layer was represented as b_{o1}. The initial values of weights and bias were created by random number generation method. Forward and backward calculations were executed repeatedly on all data pairs obtained at input and output layers until lower MSE values were achieved and final parameters of ANN model were used to predict the selected responses by using the Eq. (1)

$$Y_o = \text{logsig}\left\{w_{oh} \times \left[\text{logsig}\left(w_{hi} \times x + b_{h1}\right)\right] + b_{o1}\right\}$$

1

The relative influence of each parameter process on the response was calculated as per the method described in osmotic dehydration of banana (K. Dash et al., 2020) and microwave vacuum drying (Khawas et al., 2016).

The output parameters of the proposed ANN model were fed into the genetic algorithm as the initial population for optimizing the process, illustrated in Fig. 2. The methodology of GA works on the fundamentals of biological evolution, i.e., on the “survival of the fittest” and “natural selection” strategy. The initial population was used in the proposed fitness function (Eq. 2), and the optimized condition will be selected by the subsequent selection, crossover, and mutation, shown in Fig. 2.

$$FF = \begin{cases} \max Y_1\left(X_1, X_2, X_3, X_4\right) \\ \max Y_2\left(X_1, X_2, X_3, X_4\right) \\ \min Y_3\left(X_1, X_2, X_3, X_4\right) \\ \min Y_4\left(X_1, X_2, X_3, X_4\right) \\ 1g \le X_1 \le 5g \\ 1g \le X_2 \le 5g \\ 1g \le X_3 \le 5g \\ 100W \le X_4 \le 300W \end{cases}$$

2

2.5 Encapsulation efficiency

The encapsulation efficiency is defined as the ratio of betacyanin content inside the encapsulate to the original betacyanin content. The betacyanin content was determined using the method followed for ultrasound assisted extract from dragon fruit peel (G. V.S. Bhagya Raj & Dash, 2020b). The encapsulation efficiency was calculated by using Eq. (3).

$$\text{Encapsulation efficiency } (\backslash\%) = \frac{Be_{final}}{Be_{initial}} \times 100 \quad (3)$$

where Be_{final} is the absorbance of the sample after dissolution; $Be_{initial}$ is the initial absorbance of the sample.

2.6 Antioxidant activity

The antioxidative activity of freeze dried encapsulated dragon fruit peel was determined using DPPH assay (Šturm et al., 2019). Concisely, the encapsulated powder was added to the distilled water in the concentration of 0.5 mg/mL, and 0.1 mL of this solution was mixed with 2.9 mL of 0.1 nM solution of DPPH solution in ethanol of 96% purity. The mixture was kept at incubation for 30 mins followed by measurement of absorbance at 517 nm using a UV–vis Spectrophotometer. The blank was prepared with distilled water instead of encapsulated solution, and the antioxidant activity was calculated using Eq. (4).

$$\%\text{DPPHantioxidantcapacity}\left(Y_2\right) = \left(1 - \frac{A_{sample}}{A_{control}}\right) \times 100$$

4

$A_{control}$ = mixture of ethanol and DPPH solution, A_{sample} = solution containing encapsulation powder and DPPH solution.

2.7 Hygroscopicity

The hygroscopicity of samples was determined by placing around 0.2 g of freeze-dried encapsulate powder in a Petrie dish and storing it for one week in a descicator containing saturated NaCl (RH 75%). After one week, the samples were weighed, and hygroscopicity was calculated as g of water absorbed per 100 g of sample (%) (Yamashita et al., 2017).

2.8 Solubility

The solubility of encapsulated powder was determined according to the process followed by Wang et al., 2020 (H. Wang et al., 2020). Briefly, about 0.5g weight of encapsulated powder was added to 50 mL of distilled water present in a conical flask. The conical flask was kept in an orbital shaker at 100 rpm for 30 min at 25°C for homogenizing the mixture. After 30 min, the mixture was centrifuged at 3500 rpm for 5 min, and the supernatant was weighed ($w_{initial}$) and dried in a hot air oven at 105°C for 5 h. The dried supernatant was weighed after drying and used in Eq. (5) to calculate solubility.

$$\text{solubility} = \frac{\text{w}_{\text{initial}}}{\text{w}_{\text{final}}} \times 100$$

5

2.9 Thermal stability of freeze-dried encapsulated dragon fruit peel powders

The thermal stability of the encapsulated product was determined at two pH concentrations of 3.6 (citric acid buffer) and 7 (phosphate buffer) at a temperature of 80°C (Tao et al., 2017). The encapsulated powder (0.5g) was dissolved in 50 mL of 0.1 mol/L citric acid buffer for pH 3.6 and phosphate buffer solution for pH 7. Any changes in the pH of the solution were adjusted after the addition of encapsulated powder. The solution was maintained at 80°C in a water bath after the adjustments. The total betacyanin content of the solution was measured after 10, 20, 30, 45, 60, and 90 minutes. The data was fitted to a first order reaction using Eq. (6), and the betacyanin half-life period was estimated using Eq. (7).

$$C_t = C_0 \exp(-kt)$$

6

$$t_{1/2} = 0.693/k$$

7

Where t is time (min), C_0 is the initial betacyanin content (mg/g), C_t is the betacyanin content at time t (mg/g), k is the first order kinetic constant ($\min^{-1}$) and $t_{1/2}$ is half life time (min).

2.10 Statistical Analysis

The statistical analysis used in the present study for validating the adequacy of the model were the coefficient of determination (R^2) using Eq. (8), root mean square error (RMSE) using Eq. (9), chi-square (χ^2) using Eq. (10) and relative deviation percentage using Eq. (11) (Gurajala V.S. Bhagya Raj & Dash, 2021).

$$R^2 = 1 - \frac{\sum_{i=1}^{n}(\text{Y}_\text{p} - \text{Y}_\text{e})}{\sum_{i=1}^{n}(\text{Y}_a - \text{Y}_\text{e})} \quad (8)$$

$$\text{RMSE} = \sqrt{\frac{\sum_{i=1}^{n}(\text{Y}_\text{p} - \text{Y}_\text{e})}{\text{n}-1}} \quad (9)$$

$$\chi^2 = \frac{\sum_{i=1}^{n}\left(\text{Y}_\text{p} - \text{Y}_\text{e}\right)^2}{\text{Y}_\text{e}} \quad (10)$$

$$\text{R}_\text{d} = \frac{100}{\text{n}-1}\sum_{i=1}^{n}\frac{\left|\text{Y}_\text{e} - \text{Y}_\text{p}\right|}{\text{Y}_\text{e}} \quad (11)$$

where Y_p is the predicted value from the model, Y_e is the observed value or experimental values, Y_a is the average response value, and n is the number of experiments conducted.

3. Results And Discussions

3.1 Artificial neural network modeling of encapsulation process

The artificial neural network was implemented to simulate the encapsulation process and predict the responses based on various combinations of independent variables. The neurons in the hidden layer were chosen based on the lower MSE value obtained for training data, and the optimal ANN topology was found to be 4-11-4 with 11 neurons in the hidden layer. The selected ANN topology resulted R^2 value higher than 0.989 and MSE value lower than 0.01 for training, testing, and validation data after completion of 5000 cycles. The matrix size for the weights between input and hidden layer (w_{hi}) was 11×4 and for the weights between hidden and output layer (w_{oh}) was 4×11. The final bias matrix at hidden (b_{h1}) and output layer (b_{o1}) was a column matrix with sizes 11×1 and 4×1, respectively.

The output at the hidden layer and output layer was represented as o_h and y_o respectively, where subscript h and o represented the neuron number for the corresponding layers. The output of the output layer can be calculated using the hidden layer output, weights between the hidden and output layer, and bias at the output layer. The equation for output at the hidden layer was presented in Eq. (12).

$$y_o = logsig\left(w_{oh} \times o_h + b_{o1}\right) = \frac{1}{1 + \exp[-(w_{oh} \times o_h + b_{o1})]}$$

12

The output for the first neuron y_1 (encapsulation efficiency) was calculated by applying log sigmoid function to the value obtained after multiplying the first row of w_{oh} i.e., w_{1h} having matrix size of 1×11 with the output of hidden layer (o_h) having matrix size of 11×1 then added to the first row of bias matrix b_{o1} at the output layer, i.e., b_{11}. The equation for calculating y_1 was represented in Eq. (13).

$$y_1 = logsig\left(w_{1h} \times o_h + b_{11}\right) = \frac{1}{1 + \exp[-(w_{1h} \times o_h + b_{11})]}$$

13.1

$$w_{1h} \times o_h + b_{11} = 0.247 \times O_5 - 0.289 \times O_2 - 0.17 \times O_3 - 0.439 \times O_4 - 4.69 \times O_1 + 2.52 \times O_6 - 0.847 \times O_7 + 6.15 \times O_8 - 2.24 \times O_9 + 1.15 \times$$

13.2

Similarly, the output for the second, third and fourth neuron of the output layer was calculated using the corresponding row of w_{oh} and b_{o1}. The equations for the second, third and fourth neurons were presented in Eq. (14) to Eq. (16).

$$y_2 = logsig\left(w_{2h} \times o_h + b_{21}\right) = \frac{1}{1 + \exp[-(w_{2h} \times o_h + b_{21})]}$$

14.1

$$w_{2h} \times o_h + b_{21} = 1.91 \times O_2 - 2.75 \times O_1 - 1.29 \times O_3 - 0.244 \times O_4 + 2.28 \times O_5 + 1.9 \times O_6 - 4.13 \times O_7 + 6.34 \times O_8 - 2.73 \times O_9 + 0.231 \times O_{1(}$$

14.2

$$y_3 = logsig\left(w_{3h} \times o_h + b_{31}\right) = \frac{1}{1 + \exp[-(w_{3h} \times o_h + b_{31})]}$$

15.1

$$w_{3h} \times o_h + b_{31} = 3.93 \times O_2 - 2.21 \times O_1 - 3.08 \times O_3 - 2.83 \times O_4 - 0.176 \times O_5 + 6.9 \times O_6 + 3.01 \times O_7 - 1.6 \times O_8 + 0.895 \times O_9 - 2.2 \times O_{10} +$$

15.2

$$y_4 = logsig\left(w_{4h} \times o_h + b_{41}\right) = \frac{1}{1 + \exp[-(w_{4h} \times o_h + b_{41})]}$$

16.1

$$w_{4h} \times o_h + b_{41} = 4.49 \times O_2 - 4.13 \times O_1 + 1.86 \times O_3 - 0.915 \times O_4 + 0.108 \times O_5 - 2.11 \times O_6 - 3.59 \times O_7 + 0.808 \times O_8 + 0.00238 \times O_9 + 5.07$$

16.2

The output for each of the hidden layer neurons (Eq. 17) was calculated using the weights between input and hidden layer w_{hi} (11×4), independent variable matrix x (4×1) and bias at the hidden layer b_{h1} (11×1).

$$O_h = logsig\left(H_h\right) = logsig\left(w_{hi} \times x + b_{h1}\right) = \frac{1}{1 + \exp[-(w_{1i} \times x + b_{11})]}$$

17

The output for the first hidden layer neuron was calculated by applying log sigmoid function to the product of the first row of w_{hi} i.e., w_{1i} (1×4) and x (4×1) then added to the first row of bias at the hidden layer b_{h1} i.e., b_{11} (1×1). The equation for the output generated for the first neuron in the hidden layer was represented in Eq. (18).

$$O_1 = logsig\left(H_1\right) = logsig\left(w_{1i} \times x + b_{11}\right) = \frac{1}{1 + \exp[-(w_{1i} \times x + b_{11})]}$$

18.1

$$H_1 = w_{1i} \times x + b_{11} = 7.57 \times x_1 - 4.8 \times x_2 + 5.77 \times x_3 + 1.19 \times x_4 - 4.36$$

18.2

A similar procedure was followed for calculating the output of other neurons in the hidden layer (2 to 11) and represented from Eq. (19) to Eq. (28).

$$H_2 = 0.386 \times x_1 - 0.834 \times x_2 + 6.99 \times x_3 + 0.0154 \times x_4 - 3.74$$

19

$$H_3 = 2.51 \times x_1 + 4.18 \times x_2 + 1.65 \times x_3 - 5.31 \times x_4 - 1.04$$

20

$$H_4 = 4.75 \times x_3 - 0.767 \times x_2 - 2.59 \times x_1 + 1.96 \times x_4 - 0.188$$

21

$$H_5 = 0.784 \times x_2 - 3.35 \times x_1 + 3.51 \times x_3 - 1.43 \times x_4 - 0.516$$

22

$$H_6 = 3.72 \times x_2 - 0.131 \times x_1 + 0.818 \times x_3 - 0.317 \times x_4 - 2.07$$

23

$$H_7 = 3.9 \times x_3 - 2.42 \times x_2 - 0.825 \times x_1 + 4.11 \times x_4 - 1.05$$

24

$$H_8 = 4.09 \times x_1 - 0.42 \times x_2 + 5.57 \times x_3 - 2.01 \times x_4 - 3.5$$

25

$$H_9 = 4.4 \times x_2 - 2.03 \times x_1 - 2.63 \times x_3 + 1.75 \times x_4 - 2.19$$

26

$$H_{10} = 1.58 \times x_1 + 0.531 \times x_2 + 1.32 \times x_3 + 4.15 \times x_4 - 1.31$$

27

$$H_{11} = 2.63 \times x_1 + 3.24 \times x_2 - 6.24 \times x_3 + 6.96 \times x_4 + 1.54$$

28

3.2 Effect of process parameters on encapsulation efficiency

An effective encapsulation technique relies on attaining the maximum holding of the targeted compounds and the lowest amount of the core compounds on the surface of encapsulated powder molecules. The encapsulation efficiency for different combinations of process parameters was varied from 56.680 to 88.935%. The high yield for Y_1 was obtained at maltodextrin of 4 g, gum arabic of 4 g, gelatin of 4 g, and ultrasound power of 150 W, whereas the lowest yield of Y_1 was found at the combination of X_1 of 3g, X_2 of 1 g, X_3 of 3g and X_4 of 200 W. The plot between the experimental and predicted Y_1 of freeze-dried encapsulated product with r value of 0.98 suggest that both data were in good agreement with each other (Fig. 3(i)). The influence of process parameters X_1 on encapsulation efficiency was studied by keeping the other three process parameters at the center level and presented in Fig. 4(i). It was observed that increasing the maltodextrin content in the wall material from 1 to 3 g resulted in a steep increase in encapsulation efficiency, and further increase to 5g resulted in a slower rate of increase (Fig. 4(i)). Similarly, the influence of X_2, X_3 and {\text{X}}_{4} on encapsulation efficiency was studied by keeping the other three process parameters at the center level and shown in Fig. 4(ii), Fig. 4(iii), and Fig. 4(iv), respectively.

The calculated and predicted relative influence of each process variable on encapsulation efficiency is shown in Table (1). The quantity of gum arabic (0.495) in the encapsulation wall material has the greatest influence on encapsulation efficiency among all four process factors, followed by the quantities of gelatin (0.332), maltodextrin (0.329), and ultrasonication power (-0.281) (Table 1). Comparable results were reported when maltodextrin and gum arabic were used individually as wall material for entrapping polyphenols from fermented waste water of miang processing by freeze drying encapsulation technique with 10:1 core to wall material. The encapsulated powder with gum arabic resulted in a better encapsulation efficiency (99.35 percent) than the encapsulated powder formed with maltodextrin (89.63 percent) (Muangrat et al., 2019). Similar results of a greater effect of gum arabic on encapsulation efficiency were reported during norbixin encapsulation by spray-drying using maltodextrin and gum arabic as wall materials, where the addition of gum arabic to maltodextrin increased encapsulation efficiency from 22.52–50.02% (Tupuna et al., 2018). Minimum encapsulation efficiency was reported while using only maltodextrin for wall material. This might be due to the typical characteristics of polymers, such as very low surface activity, the inadequacy of emulsification, and poor ability to form films, hence maltodextrin is generally combined with compounds with good emulsifying capabilities (Cano-Higuita et al., 2015). Gum arabic is a highly branched heteropolymer of sugars built by a ramified carbohydrate chain and minor glycoproteins connected by covalent bonds. This favors gum arabic to combine with both hydrophilic and hydrophobic molecules in nature, and thus it is a magnificent emulsifying agent in an extensive range of pH. Hence gum arabic is suitable with a vast range of polymers and entraps the targeted molecule because of its great ability to form films (Akhavan Mahdavi et al., 2016). The three components of blends for wall material, i.e., gum arabic, maltodextrin, and gelatin found to have a positive effect on {\text{Y}}_{1} whereas ultrasound power has a negative effect. The logic behind the positive impact of wall material components can be associated with the great solubility of the component blends of targeted compounds and the low viscosity when a high composition of solids are used (Özkan & Ersus Bilek, 2014). The encapsulation efficiency of spray-dried encapsulated product formed from the pulp of Juçara (Euterpe edulis M.) using maltodextrin, gum arabic, and gelatin as wall material was found to be 83% (Bicudo et al., 2015). Gelatin mixed with other polymers for encapsulation improves the color staining effect and thus enhances the stability of UAE extracted dragon fruit peel containing betacyanin. Similar results of improved stability of curcumin pigment were reported for spray-dried encapsulation method using gelatin and porous starch as wall material (Y. Wang et al., 2009).

Table 1
Relative effect of process parameters on the properties of freeze-dried encapsulated product

Relative effect	{\mathbf{y}}_{1}	{\mathbf{y}}_{2}	{\mathbf{y}}_{3}	{\mathbf{y}}_{4}
x1\left[{\left({\text{y}}_{\text{i}}\right)}_{+\text{1,0},\text{0,0}}-{\left({\text{y}}_{\text{i}}\right)}_{-\text{1,0},\text{0,0}}\right]	0.329	0.695	-0.605	0.536
x2\left[{\left({\text{y}}_{\text{i}}\right)}_{0,+\text{1,0},0}-{\left({\text{y}}_{\text{i}}\right)}_{0,-\text{1,0},0}\right]	0.495	0.639	0.520	0.773
x3\left[{\left({\text{y}}_{\text{i}}\right)}_{\text{0,0},+\text{1,0}}-{\left({\text{y}}_{\text{i}}\right)}_{\text{0,0},-\text{1,0}}\right]	0.332	0.33	-0.434	-0.447
x4\left[{\left({\text{y}}_{\text{i}}\right)}_{\text{0,0},0+1}-{\left({\text{y}}_{\text{i}}\right)}_{\text{0,0},0,-1}\right]	-0.281	-0.458	0.449	0.343
Where in {\text{y}}_{\text{i}}, 'i' denotes the response neuron				

The reason for the decrease in {\text{Y}}_{1} with increase of {\text{X}}_{4} may be associated with the thermal degradation of betacyanin with the increase of power during mixing of the encapsulating agents and core material. This phenomenon might have resulted in a decrease in encapsulation efficiency. The heat produced in the solution during ultrasonication may be due to the collapsing bubbles, and this heat might have increased with the increase of ultrasonication power (Leong et al., 2017). A similar trend was reported during the encapsulation of coconut milk by spray drying with the application of ultrasound for homogenization, where the encapsulation efficiency was approximately 80% for ultrasonication power of 5.68 W/g, and a decrease of encapsulation efficiency of 12.5% was observed with the increase of power to 6.68 W/g but the increase of power from 2.27 to 5.56 W/g increased the encapsulation efficiency (Le & Le, 2015).

3.3 Effect of process parameters on antioxidant activity

The antioxidant activity was found to be in the range of 59.890 to 82.319% under the selected experimental conditions of four independent variables. The maximum antioxidant activity was observed when the {\text{X}}_{1} of 4 g, {\text{X}}_{2} of 4 g, {\text{X}}_{3} of 4 g and {\text{X}}_{4} of 150 W, and the minimum antioxidant activity was found at the independent variable combination of {\text{X}}_{1} of 3 g, {\text{X}}_{2} of 1 g/100ml, {\text{X}}_{3} of 3 g and {\text{X}}_{4} of 200 W. The output of antioxidant activity of freeze-dried encapsulated product data obtained by the ANN model equation formed in Eq. (14) was plotted against the observed antioxidant data of freeze-dried dragon fruit peel encapsulated product (\text{r}=0.98) and shown in Fig. 3(ii).

From the ANN modeling, the sequence of the relative effect of process parameters was as follows {\text{X}}_{1} (0.695), {\text{X}}_{2} (0.639), {\text{X}}_{4} (-0.458) and {\text{X}}_{3} (0.330), shown in Table 1. Out of all the four process parameters, ultrasound power was found to have a negative effect on antioxidant activity. The three process parameters are the components of wall material found to have a positive effect, shown in Table 1. The effect of process parameters on antioxidant activity was similar to that of encapsulation efficiency of the freeze-dried encapsulated product.

The antioxidant activity of freeze-dried encapsulated powder was affected higher by {\text{X}}_{1} compared with the other three independent variables. Similar trends of the higher effect of maltodextrin were reported during encapsulation of eggplant peel extract by spray drying method using maltodextrin and gum arabic as wall material with core to wall ratio of 1:1. The reported antioxidant activity of encapsulated egg plant peel while using maltodextrin, gum arabic, and a combination of both components as wall materials was 71.25%, 55.73%, and 63.52%, respectively (Sarabandi et al., 2019).

Using freeze drying method for encapsulating of spent coffee grounds with maltodextrin as wall material reported antioxidant activity (FRAP assay) of 1.56 mmol Fe(II)/100ml while the change in wall material to gum arabic the antioxidant activity was decreased by 22.44% (Ballesteros et al., 2017). The results suggested that the use of a higher composition of {\text{X}}_{1} in wall material was more appropriate for preserving the antioxidant activity of bioactive compounds while applying freeze drying technique for encapsulation of bioactive compounds.

The positive effect of gum arabic on the response {\text{Y}}_{2} of encapsulated product can be associated to the chemical structure of protein fraction in gum arabic (Tonon et al., 2010). A similar trend of increase in antioxidant activity from 84 to 89% was observed with the increase of gum arabic in core to gum arabic ratio from 1:4 to 1:6 during spray drying of propolis (Da Silva et al., 2013).

The positive effect of {\text{X}}_{3} on the antioxidant activity may be due to the interaction with the maltodextrin at temperatures produced during ultrasonication resulting in Maillard reaction forming melanoidins. Melanoidins formed by this process tend to have high molecular weight and antioxidant activity (H. Y. Wang et al., 2011). The application of ultrasound power might have affected the antioxidant property in a negative way due to the heat produced in the mixture, as the ultrasound is mainly mechanical and the vibration of product structure caused by ultrasound application can convert this mechanical energy into heat by friction (Colucci et al., 2018). The ultrasound power has increased antioxidant activity of encapsulated product with an increase of power from 100 to 150 W, but further increase in ultrasound power demonstrated a decline in antioxidant activity, which can be visualized from Fig. 4(iv).

3.4 Effect of process parameters on hygroscopicity

Hygroscopicity is chiefly influenced by inherent compositions of product, the physical structure of product like surface area and particle morphology, and also on concentrations of the drying carriers and drying methods (Arshad et al., 2020; Ferrari et al., 2012). It helps in determining the shelf life and stability of the dried products where the powder is considered non hygroscopic if the hygroscopicity value is less than 10%. One approach to reduce the hygroscopicity of bioactive compound powder is by encapsulating it with high molecular weight wall materials (Bhandari et al., 2013). The high {\text{Y}}_{3} value of 8.699 g/100g was found for the encapsulated product that formed with wall material prepared by the combination of {\text{X}}_{1}, {\text{X}}_{2} and {\text{X}}_{3} of 2 g, 4 g/100ml, and 4 g and the core to wall ratio of 250 W and respectively.

The low {\text{Y}}_{3} value of 6.334 g/100g was observed for the encapsulated product formed with the wall material containing {\text{X}}_{1} of 5 g, {\text{X}}_{2} of 3 g and {\text{X}}_{3} of 3 g when homogenized at ultrasound power ({\text{X}}_{4}) of 200 W. The predicted and the experimental hygroscopic data at different combinations of process parameters were found to be in good agreement with each other suggested by a higher r value of 0.98 and were pictorially represented in Fig. 3(iii). The influence of process parameters on the hygroscopicity of the encapsulated product was illustrated in Fig. 4. From the relative effect of process parameters, it was found that {\text{X}}_{3} having less effect on {\text{Y}}_{3} compared with the other three process parameters. {\text{X}}_{1} found to have a higher effect on the hygroscopicity, the relative effect of the four process parameters was as follows {\text{X}}_{1} \left(-0.605\right)>{\text{X}}_{2} \left(0.520\right)>{\text{X}}_{4} \left(0.449\right)>{\text{X}}_{3}(-0.434). The {\text{X}}_{2} and {\text{X}}_{4} found to have a positive effect on hygroscopicity that means increase of these parameters showed increase in the {\text{Y}}_{3} whereas the {\text{X}}_{1} and {\text{X}}_{3} found to have negative effect on the {\text{Y}}_{3} illustrates the increase in the value of these parameters decreased the response {\text{Y}}_{3}. The negative effect of maltodextrin on the hygroscopicity can be attributed to its ability to enhance the stability of the dried encapsulated powder due to its less hygroscopicity nature and high molecular weight of maltodextrin (W. Wang & Zhou, 2012). The hygroscopicity of freeze dried encapsulated product from Averrhoa carambola pomace was also reported to decrease from 6.83 to 5.55 with the increase of maltodextrin content from 10–20% in wall material (Saikia et al., 2015). Similar results of decrease in hygroscopicity were observed with increase of maltodextrin from 5–15% while encapsulating the beetroot juice with spray drying technique (Bazaria & Kumar, 2018) and the hygroscopicity of spray dried encapsulated product was also reported to decrease with increase of maltodextrin (Rodríguez-Hernández et al., 2005). The increased level of {\text{X}}_{2} in turn, increased the hygroscopicity of encapsulated product can be associated with easier polar interaction between its hydrogen chain and water due to different polarity and the highly branched structure of the gum arabic. A similar pattern of increase in hygroscopicity from 9.18–10.66% was observed with the increase of gum arabic from 0–2% in wall material along with maltodextrin during spray dried encapsulation of propolis extract (Sukri et al., 2021). Results reported for microwave-assisted encapsulated anthocyanins from Ipomoea batatas showed that the product with only maltodextrin, only gum arabic and combination of both as wall material was found to have low hygroscopicity value of 10.028, high hygroscopicity value of 18.736 and moderate hygroscopicity value of 15.181 respectively (Mohd Nawi et al., 2015). The composition of gelatin was found to have a negative effect on the hygroscopicity of the encapsulated product, i.e., increase in {X}_{3} composition in the wall material decreased the hygroscopicity. Similar results of decrease in hygroscopicity from 49.05 to 45.25 g/100g was observed with increase of gelatin content and gum Arabic content from 5 to 7 (v/v) with 50% of core material during encapsulation of anthocyanins form black raspberry by freeze drying method (Shaddel et al., 2018).

3.5 Effect of process parameters on solubility

Solubility is the most reliable parameter to assess the characteristics of dried powder in an aqueous solution, whether to form a solution or suspension in water. Higher {\text{Y}}_{4} of 52.805% was found for the encapsulated product that formed when the {\text{X}}_{4} was 250 W and wall material constitutes of {\text{X}}_{1}, {\text{X}}_{2} and {\text{X}}_{3} of 4 g, 4 g and 2 g, respectively. The lowest {\text{Y}}_{4} of 27.003% was observed for the process parameter combination of {\text{X}}_{1}, {\text{X}}_{2}, {\text{X}}_{3} and {\text{X}}_{4} of 1 g, 3 g, 3 g, and 200 W, respectively. The effect of independent variables of the process on the dependent variable of the process is shown in Fig. 4. The observed and the ANN predicted values for {\text{Y}}_{4} was plotted and found to have r value of 0.99, illustrated in Fig. 3(iv).

Gum Arabic composition ({\text{X}}_{2}) in wall material found to have a higher effect on solubility followed by {\text{X}}_{1}, {\text{X}}_{3} and {\text{X}}_{4}, the sequence of process variables from high to low effect as follows {\text{X}}_{2}\left(0.773\right)>{\text{X}}_{1}\left(0.536\right)>{\text{X}}_{3}(-0.447)> {\text{X}}_{4}\left(0.343\right). The response {\text{Y}}_{4} was increased with the increase of {\text{X}}_{1}, {\text{X}}_{2} and {\text{X}}_{4} which was justified by the relative effect illustrated in Table 1, while the {\text{X}}_{3} found to have a negative effect on the response {\text{Y}}_{4} of freeze-dried encapsulated product. The positive effect of hydrolyzed starch such as maltodextrin on the solubility of the encapsulated product was due to lower-molecular-weight complexes resulting from the depolymerization of native starch. The increase in solubility of spray-dried encapsulated betacyanins was reported when maltodextrin was used as wall material (Cai & Corke, 2000).

The higher effect of gum arabic on solubility can be associated with high water solubility and the ability to produce low viscosity solutions at high concentrations of solids than other gums (Madene et al., 2006).

An increase of gelatin content in the wall material component influenced the solubility of encapsulated product negatively; this may be due to the formation of a coating, which delayed the leaching of low molecular weight compounds. The results were supported by the increase in solubility time of the encapsulated product of turmeric oleoresin with an increase of gelatin content in the wall material when the maltodextrin was kept constant (Malacrida & Telis, 2011). A similar trend of decrease in solubility in cold water was reported for freeze dried microencapsulated beta-carotene with increase of gelatin content in wall material when used along with starch (Spada et al., 2012). The low frequency high intensity ultrasound generates strong shear and mechanical forces (Leong et al., 2018; Yang et al., 2020), these forces might have influenced the mixing of the wall materials and core components in a positive way and in turn proper mixing of components increased the solubility of encapsulated product.

3.6 Optimization and validation of combined ANN-GA model

The process parameters of the freeze-drying encapsulation of UAE extracted dragon fruit peel was optimized by using GA. The input or the objective function for the GA optimization was the equations formed by using the parameters of ANN model, which are weights and bias. The fitness functions of the GA were presented in Eq. (2), and this function provides a set of 18 solutions. From these solutions, the optimized condition was found to {\text{X}}_{1} of 4.461 g, {\text{X}}_{2} of 3.863 g, {\text{X}}_{3} of 3.198 g and {\text{X}}_{4} of 123 W according to the highest fitness value using Eq. (2). The predicted values for the responses {\text{Y}}_{1}, {\text{Y}}_{2}, {\text{Y}}_{3} and {\text{Y}}_{4} at the optimized condition was found to be 88.143%, 81.702%, 6.924 g/100g, and 32.841%, respectively. For the validation of the proposed model, the experiment was conducted at the optimum condition {\text{X}}_{1} of 4.5 g, {\text{X}}_{2} of 3.9 g, {\text{X}}_{3} of 3.2 g and {\text{X}}_{4} of 120 W, and the observed values for responses at this condition was found to be 89.715%, 80.039%, 7.003

g/100g, and 32.418% for {\text{Y}}_{1}, {\text{Y}}_{2}, {\text{Y}}_{3} and {\text{Y}}_{4} respectively. The relative deviation between the predicted and observed responses was calculated using Eq. (11) and found to be less than 2.077%, presented in Table 2.

Table 2.ANN-GA model predicted responses and experimental values at the optimum condition

Response ⟶	Encapsulation efficiency (%)	Antioxidant activity (%)	Hygroscopicity (g/100g)	Solubility (%)
Predicted	88.143	81.702	6.924	32.841
Experimental	89.715	80.039	7.003	32.418
Relative deviation (%)	1.752	2.077	1.129	1.305

3.7 Thermal stability study of freeze-dried encapsulated dragon fruit peel powder

The thermal stability of freeze-dried encapsulated dragon fruit peel powder was studied at two different pH 7 and 3.6 at temperature of 80°C in terms of betacyanin content. The linear degradation of betacyanin with respect to time at two pH levels followed first order kinetic model, and the data were fitted with Eq. (6), illustrated in Fig. 5. Similarly first order kinetic model was used to study the degradation kinetics of spray-dried encapsulated blueberry powder in terms of anthocyanins (Tao et al., 2017). The first order kinetic model fitted the experimental data with higher {R}^{2} (> 0.977) and lower values for errors {\chi }^{2} (< 9.981) and RMSE (< 2.925), presented in Table 3. The amount of betacyanin retained for the sample treated at pH 7 and 3.6 was found to be 68.485% and 60.135%, respectively. The highest retention was found for the sample treated at pH 7 with the lowest first order kinetic parameter (k) of value 0.495\times {10}^{-2}, {\text{m}\text{i}\text{n}}^{-1}. From the table, it can be observed that a decrease in pH from 7 to 3.6 increased the degradation rate constant by 35.152%. Comparable results were found where an increase in k value was observed with the decrease of pH while studying the thermal stability of

Table 3
Thermal stability of freeze-dried encapsulated product at 80°C and two pH levels

pH	\mathbf{k}\times {10}^{-2}, {\mathbf{m}\mathbf{i}\mathbf{n}}^{-1}	{\mathbf{t}}_{1/2}, min	{\mathbf{R}}^{2}	{{\chi }}^{2}	RMSE
7	0.495\pm 0.009	140.030\pm 1.372	0.977	5.887	2.246
3.6	0.669\pm 0.015	103.609\pm 1.165	0.989	9.981	2.925

The half-life time was calculated using Eq. (7) and presented in Table 3. The half-life time for the sample treated with pH of 3.6 was found to be 103 min, and an increase in pH to 7 increased the half-life time to 140 min. These results demonstrate that the freeze-dried encapsulated product was more stable at pH of 7 than the pH of 3.6 when treated at 80°C temperature, shown in Table 4. Half-life time is inversely proportional to the first order rate constant, i.e., an increase in k value decreases the {t}_{1/2} value.

4. Conclusion

In this study, the ultrasound assisted extracted dragon fruit peel was encapsulated using the freeze drying technique, and the process was modeled and optimized using integrated ANN-GA. The properties evaluated for the freeze-dried encapsulated powder at different combinations of process parameters were encapsulation efficiency, antioxidant activity, hygroscopicity, and solubility. At different combinations of process parameters the encapsulation efficiency, antioxidant activity, hygroscopicity, and solubility was found to be in the range of 56.680–88.935%, 59.890–82.319%, 6.334–8.699 g/100g, and 27.003–52.805%, respectively. The optimized concentration of maltodextrin, gum arabica, and gelatin was 6.22 g, 3.74 g, and 1.04 g, respectively. The optimum ultrasonic power was found to be 132 W. The predicted values of encapsulation efficiency (%), antioxidant activity (%), hygroscopicity (g/100g), and solubility (%) were 88.143, 81.702, 6.924, and 32.841, respectively. The relative deviation between the predicted and experimental value at optimum conditions was found to be less than 2.077%. The data for thermal stability of encapsulated powder at 80°C and two pH of 7 and 3.6 followed first order kinetic model, and the rate constant was 0.495 ± 0.009 and 0.669 ± 0.015 \text{m}\text{i}{\text{n}}^{-1} respectively. The encapsulated powder was more thermally stable at 80°C and pH 7 than the powder treated at pH 3.6. It was validated by half-life times of 140 and 103 minutes for pH 7 and 3.6, respectively. The freeze dried encapsulated powder obtained by this approach increased heat stability and had the capacity of controlled release, and the encapsulation matrix acted as an ideal vehicle for antioxidant delivery.

Declarations

Author Contributions Statement

G.V.S. Bhagya Raj and Kshirod K. Dash wrote the main manuscript text, prepared figures and tables.Kshirod K. Dash reviewed the manuscript.

Data Availability

All data and materials are availableupon reasonable request from the corresponding author.

Ethics Approval:

Not applicable.

Consent to Participate:

Not applicable.

Consent for Publication:

Not applicable.

Conflict of Interest:

The authors declare that they have no conflict of interest.

References

1. Akhavan Mahdavi, S., Jafari, S. M., Assadpoor, E., & Dehnad, D. (2016). Microencapsulation optimization of natural anthocyanins with maltodextrin, gum Arabic and gelatin. *International Journal of Biological Macromolecules*, *85*, 379–385. https://doi.org/10.1016/j.ijbiomac.2016.01.011
2. Al-Mekhlafi, N. A., Mediani, A., Ismail, N. H., Abas, F., Dymerski, T., Lubinska-Szczygeł, M., Vearasilp, S., & Gorinstein, S. (2021). Metabolomic and antioxidant properties of different varieties and origins of Dragon fruit. *Microchemical Journal*, *160*. https://doi.org/10.1016/j.microc.2020.105687
3. Aliakbarian, B., Sampaio, F. C., de Faria, J. T., Pitangui, C. G., Lovaglio, F., Casazza, A. A., Converti, A., & Perego, P. (2018). Optimization of spray drying microencapsulation of olive pomace polyphenols using Response Surface Methodology and Artificial Neural Network. *LWT*, *93*, 220–228. https://doi.org/10.1016/j.lwt.2018.03.048
4. Antigo, J. L. D., Bergamasco, R. de C., & Madrona, G. S. (2018). Effect of ph on the stability of red beet extract (Beta vulgaris l.) microcapsules produced by spray drying or freeze drying. *Food Science and Technology*, *38*(1), 72–77. https://doi.org/10.1590/1678-457x.34316
5. Arshad, H., Ali, T. M., & Hasnain, A. (2020). Comparative study on efficiency of nutmeg microencapsulation (freeze-drying method) using native and OSA sorghum starch as wall materials in combination with gum arabic. *Cereal Chemistry*, *97*(3), 589–600. https://doi.org/10.1002/cche.10275
6. Azarpazhooh, E., Sharayei, P., Zomorodi, S., & Ramaswamy, H. S. (2019). Physicochemical and Phytochemical Characterization and Storage Stability of Freeze-dried Encapsulated Pomegranate Peel Anthocyanin and In Vitro Evaluation of Its Antioxidant Activity. *Food and Bioprocess Technology*, *12*(2), 199–210. https://doi.org/10.1007/s11947-018-2195-1
7. Balendres, M. A., & Bengoa, J. C. (2019). Diseases of dragon fruit (Hylocereus species): Etiology and current management options. In *Crop Protection* (Vol. 126). https://doi.org/10.1016/j.cropro.2019.104920
8. Ballesteros, L. F., Ramirez, M. J., Orrego, C. E., Teixeira, J. A., & Mussatto, S. I. (2017). Encapsulation of antioxidant phenolic compounds extracted from spent coffee grounds by freeze-drying and spray-drying using different coating materials. *Food Chemistry*, *237*, 623–631. https://doi.org/10.1016/j.foodchem.2017.05.142
9. Bamidele, O. P., & Emmambux, M. N. (2021). Encapsulation of bioactive compounds by “extrusion” technologies: a review. In *Critical Reviews in Food Science and Nutrition* (Vol. 61, Issue 18, pp. 3100–3118). https://doi.org/10.1080/10408398.2020.1793724
10. Bazaria, B., & Kumar, P. (2018). Optimization of spray drying parameters for beetroot juice powder using response surface methodology (RSM). *Journal of the Saudi Society of Agricultural Sciences*, *17*(4), 408–415. https://doi.org/10.1016/j.jssas.2016.09.007
11. Bhagya Raj, G. V.S., & Dash, K. K. (2020a). Comprehensive study on applications of artificial neural network in food process modeling. In *Critical Reviews in Food Science and Nutrition*. https://doi.org/10.1080/10408398.2020.1858398
12. Bhagya Raj, G. V.S., & Dash, K. K. (2020b). Ultrasound-assisted extraction of phytocompounds from dragon fruit peel: Optimization, kinetics and thermodynamic studies. *Ultrasonics Sonochemistry*, *68*. https://doi.org/10.1016/j.ultsonch.2020.105180
13. Bhagya Raj, Gurajala V.S., & Dash, K. K. (2021). Heat transfer analysis of convective and microwave drying of dragon fruit. *Journal of Food Process Engineering*, *44*(9). https://doi.org/10.1111/jfpe.13775
14. Bicudo, M. O. P., Jó, J., Oliveira, G. A. de, Chaimsohn, F. P., Sierakowski, M. R., Freitas, R. A. de, & Ribani, R. H. (2015). Microencapsulation of Juçara (Euterpe edulis M.) Pulp by Spray Drying Using Different Carriers and Drying Temperatures. *Drying Technology*, *33*(2), 153–161. https://doi.org/10.1080/07373937.2014.937872
15. Böger, B. R., Acre, L. B., Viegas, M. C., Kurozawa, L. E., & Benassi, M. T. (2021). Roasted coffee oil microencapsulation by spray drying and complex coacervation techniques: Characteristics of the particles and sensory effect. Innovative Food Science & Emerging Technologies, 72, 102739.
16. Carpentier, J., Conforto, E., Chaigneau, C., Vendeville, J. E., & Maugard, T. (2021). Complex coacervation of pea protein isolate and tragacanth gum: Comparative study with commercial polysaccharides. Innovative Food Science & Emerging Technologies, 69, 102641.
17. Carpentier, J., Conforto, E., Chaigneau, C., Vendeville, J. E., & Maugard, T. (2022). Microencapsulation and controlled release of α-tocopherol by complex coacervation between pea protein and tragacanth gum: A comparative study with arabic and tara gums. Innovative Food Science & Emerging Technologies, 102951.
18. Cai, Y. Z., & Corke, H. (2000). Production and properties of spray-dried Amaranthus betacyanin pigments. *Journal of Food Science*, *65*(7), 1248–1252. https://doi.org/10.1111/j.1365-2621.2000.tb10273.x
19. Cano-Higuita, D. M., Vélez, H. A. V., & Telis, V. R. N. (2015). Microencapsulação de oleoresina de cúrcuma em misturas binárias e ternárias de goma arábica, maltodextrina e amido modificado. *Ciencia e Agrotecnologia*, *39*(2), 173–182. https://doi.org/10.1590/S1413-70542015000200009
20. Chasiotis, V. K., Tzempelikos, D. A., Filios, A. E., & Moustris, K. P. (2020). Artificial neural network modelling of moisture content evolution for convective drying of cylindrical quince slices. *Computers and Electronics in Agriculture*, *172*. https://doi.org/10.1016/j.compag.2019.105074

21. Cheng, A. W., Xie, H. X., Qi, Y., Liu, C., Guo, X., Sun, J. Y., & Liu, L. N. (2017). Effects of storage time and temperature on polyphenolic content and qualitative characteristics of freeze-dried and spray-dried bayberry powder. *LWT - Food Science and Technology*, *78*, 235–240. https://doi.org/10.1016/j.lwt.2016.12.027
22. Colucci, D., Fissore, D., Rossello, C., & Carcel, J. A. (2018). On the effect of ultrasound-assisted atmospheric freeze-drying on the antioxidant properties of eggplant. *Food Research International*, *106*, 580–588. https://doi.org/10.1016/j.foodres.2018.01.022
23. Da Silva, F. C., Da Fonseca, C. R., De Alencar, S. M., Thomazini, M., Balieiro, J. C. D. C., Pittia, P., & Favaro-Trindade, C. S. (2013). Assessment of production efficiency, physicochemical properties and storage stability of spray-dried propolis, a natural food additive, using gum Arabic and OSA starch-based carrier systems. *Food and Bioproducts Processing*, *91*(1), 28–36. https://doi.org/10.1016/j.fbp.2012.08.006
24. Dash, K., Bhagya Raj, G., & Gayary, M. (2020). Application of Neural Networks in Optimizing Different Food Processes Case Study. In *Mathematical and Statistical Applications in Food Engineering* (pp. 346–362). https://doi.org/10.1201/9780429436963-22
25. Dash, K. K., & Das, S. K. (2021). Modeling and optimization of microwave puffing of rice using artificial neural network and genetic algorithm. *Journal of Food Process Engineering*, *44*(1). https://doi.org/10.1111/jfpe.13577
26. Dima, Ş., Dima, C., & Iordăchescu, G. (2015). Encapsulation of Functional Lipophilic Food and Drug Biocomponents. In *Food Engineering Reviews* (Vol. 7, Issue 4, pp. 417–438). https://doi.org/10.1007/s12393-015-9115-1
27. Espinosa-Sandoval, L. A., Cerqueira, M. A., Ochoa-Martínez, C. I., & Ayala-Aponte, A. A. (2019). Phenolic Compound–Loaded Nanosystems: Artificial Neural Network Modeling to Predict Particle Size, Polydispersity Index, and Encapsulation Efficiency. *Food and Bioprocess Technology*, *12*(8), 1395–1408. https://doi.org/10.1007/s11947-019-02298-8
28. Faridnia, M., Mohammadi Sani, A., & Najaf Najafı, M. (2020). Encapsulation of red beetroot extract using spray drying and freeze drying by malto-dexterin and whey protein isolate carriers. *Iranian Food Science and Technology Research Journal*, *16*(2), 313–322.
29. Ferrari, C. C., Germer, S. P. M., & de Aguirre, J. M. (2012). Effects of Spray-Drying Conditions on the Physicochemical Properties of Blackberry Powder. *Drying Technology*, *30*(2), 154–163. https://doi.org/10.1080/07373937.2011.628429
30. Galves, C., Galli, G., Miranda, C. G., & Kurozawa, L. E. (2021). Improving the emulsifying property of potato protein by hydrolysis: an application as encapsulating agent with maltodextrin. Innovative Food Science & Emerging Technologies, 70, 102696.
31. Gengatharan, A., Dykes, G. A., & Choo, W. S. (2015). Betalains: Natural plant pigments with potential application in functional foods. In *Lwt* (Vol. 64, Issue 2, pp. 645–649). https://doi.org/10.1016/j.lwt.2015.06.052
32. Guo, J., Li, P., Kong, L., & Xu, B. (2020). Microencapsulation of curcumin by spray drying and freeze drying. *Lwt*, *132*. https://doi.org/10.1016/j.lwt.2020.109892
33. Herbach, K. M., Stintzing, F. C., & Carle, R. (2006). Betalain stability and degradation - Structural and chromatic aspects. In *Journal of Food Science* (Vol. 71, Issue 4). https://doi.org/10.1111/j.1750-3841.2006.00022.x
34. Hua, Q., Chen, C., Tel Zur, N., Wang, H., Wu, J., Chen, J., Zhang, Z., Zhao, J., Hu, G., & Qin, Y. (2018). Metabolomic characterization of pitaya fruit from three red-skinned cultivars with different pulp colors. *Plant Physiology and Biochemistry*, *126*, 117–125. https://doi.org/10.1016/j.plaphy.2018.02.027
35. Huang, S. M., Kuo, C. H., Chen, C. A., Liu, Y. C., & Shieh, C. J. (2017). RSM and ANN modeling-based optimization approach for the development of ultrasound-assisted liposome encapsulation of piceid. *Ultrasonics Sonochemistry*, *36*, 112–122. https://doi.org/10.1016/j.ultsonch.2016.11.016
36. Khawas, P., Dash, K. K., Das, A. J., & Deka, S. C. (2016). Modeling and optimization of the process parameters in vacuum drying of culinary banana (Musa ABB) slices by application of artificial neural network and genetic algorithm. *Drying Technology*, *34*(4), 491–503. https://doi.org/10.1080/07373937.2015.1060605
37. Le, H. Du, & Le, V. V. M. (2015). Application of ultrasound to microencapsulation of coconut milk fat by spray drying method. *Journal of Food Science and Technology*, *52*(4), 2474–2478. https://doi.org/10.1007/s13197-014-1285-y
38. Lengyel, M., Kállai-Szabó, N., Antal, V., Laki, A. J., & Antal, I. (2019). Microparticles, microspheres, and microcapsules for advanced drug delivery. In *Scientia Pharmaceutica* (Vol. 87, Issue 3). https://doi.org/10.3390/scipharm87030020
39. Leong, T. S. H., Martin, G. J. O., & Ashokkumar, M. (2017). Ultrasonic encapsulation – A review. In *Ultrasonics Sonochemistry* (Vol. 35, pp. 605–614). https://doi.org/10.1016/j.ultsonch.2016.03.017
40. Leong, T. S. H., Walter, V., Gamlath, C. J., Yang, M., Martin, G. J. O., & Ashokkumar, M. (2018). Functionalised dairy streams: Tailoring protein functionality using sonication and heating. *Ultrasonics Sonochemistry*, *48*, 499–508. https://doi.org/10.1016/j.ultsonch.2018.07.010
41. Madene, A., Jacquot, M., Scher, J., & Desobry, S. (2006). Flavour encapsulation and controlled release - A review. *International Journal of Food Science and Technology*, *41*(1), 1–21. https://doi.org/10.1111/j.1365-2621.2005.00980.x
42. Malacrida, C. R., & Telis, V. R. . (2011). Effect of Different Ratios of Maltodextrin/Gelatin and Ultrasound in The Microencapsulation Efficiency of Turmeric Oleoresin. *Proceedings of the 11th International Congress on Engineering and Food,* FPE915.
43. Mohd Nawi, N., Muhamad, I. I., & Mohd Marsin, A. (2015). The physicochemical properties of microwave-assisted encapsulated anthocyanins from Ipomoea batatas as affected by different wall materials. *Food Science and Nutrition*, *3*(2), 91–99. https://doi.org/10.1002/fsn3.132
44. Morales, N. X. C., Gómez, K. Y. V., Schweiggert, R. M., & Delgado, G. T. C. (2021). Stabilisation of betalains and phenolic compounds extracted from red cactus pear (Opuntia ficus-indica) by spray and freeze-drying using oca (Oxalis tuberosa) starch as drying aid. *Food Science and Technology International*, *27*(5), 456–469. https://doi.org/10.1177/1082013220963973
45. Muangrat, R., Ravichai, K., & Jirarattanarangsri, W. (2019). Encapsulation of polyphenols from fermented wastewater of Miang processing by freeze drying using a maltodextrin/gum Arabic mixture as coating material. *Journal of Food Processing and Preservation*, *43*(4). https://doi.org/10.1111/jfpp.13908

46. Nafiunisa, A., Aryanti, N., Wardhani, D. H., & Kumoro, A. C. (2017). Microencapsulation of Natural Anthocyanin from Purple Rosella Calyces by Freeze Drying. *Journal of Physics: Conference Series*, *909*(1). https://doi.org/10.1088/1742-6596/909/1/012084
47. Özkan, G., & Ersus Bilek, S. (2014). Microencapsulation of Natural Food Colourants. *International Journal of Nutrition and Food Sciences*, *3*(3), 145. https://doi.org/10.11648/j.ijnfs.20140303.13
48. Ozkan, G., Franco, P., De Marco, I., Xiao, J., & Capanoglu, E. (2019). A review of microencapsulation methods for food antioxidants: Principles, advantages, drawbacks and applications. *Food Chemistry*, *272*, 494–506. https://doi.org/10.1016/j.foodchem.2018.07.205
49. Przybył, K., Gawałek, J., Koszela, K., Wawrzyniak, J., & Gierz, L. (2018). Artificial neural networks and electron microscopy to evaluate the quality of fruit and vegetable spray-dried powders. Case study: Strawberry powder. *Computers and Electronics in Agriculture*, *155*, 314–323. https://doi.org/10.1016/j.compag.2018.10.033
50. Rahayuningsih, E., Subagya, I. S., Setiawan, F. A., & Petrus, H. T. B. M. (2019). Fresh Neem Leaves (Azadirachta indica A. Juss) extraction and application: An Optimization using Response Surface Methodology. *Asian Journal of Chemistry*, *31*(11), 2567–2574. https://doi.org/10.14233/ajchem.2019.22207
51. Rahayuningsih, Edia, Setiawan, F. A., Rahman, A. B. K., Siahaan, T., & Petrus, H. T. B. M. (2021). Microencapsulation of betacyanin from red dragon fruit (Hylocereus polyrhizus) peels using pectin by simple coacervation to enhance stability. *Journal of Food Science and Technology*, *58*(9), 3379–3387. https://doi.org/10.1007/s13197-020-04910-8
52. Rezende, Y. R. R. S., Nogueira, J. P., & Narain, N. (2018). Microencapsulation of extracts of bioactive compounds obtained from acerola (Malpighia emarginata DC) pulp and residue by spray and freeze drying: Chemical, morphological and chemometric characterization. *Food Chemistry*, *254*, 281–291. https://doi.org/10.1016/j.foodchem.2018.02.026
53. Rodríguez-Hernández, G. R., González-García, R., Grajales-Lagunes, A., Ruiz-Cabrera, M. A., & Abud-Archila, M. (2005). Spray-drying of cactus pear juice (Opuntia streptacantha): Effect on the physicochemical properties of powder and reconstituted product. *Drying Technology*, *23*(4), 955–973. https://doi.org/10.1080/DRT-200054251
54. Saikia, S., Mahnot, N. K., & Mahanta, C. L. (2015). Optimisation of phenolic extraction from Averrhoa carambola pomace by response surface methodology and its microencapsulation by spray and freeze drying. *Food Chemistry*, *171*, 144–152. https://doi.org/10.1016/j.foodchem.2014.08.064
55. Sarabandi, K., Jafari, S. M., Mahoonak, A. S., & Mohammadi, A. (2019). Application of gum Arabic and maltodextrin for encapsulation of eggplant peel extract as a natural antioxidant and color source. *International Journal of Biological Macromolecules*, *140*, 59–68. https://doi.org/10.1016/j.ijbiomac.2019.08.133
56. Shaddel, R., Hesari, J., Azadmard-Damirchi, S., Hamishehkar, H., Fathi-Achachlouei, B., & Huang, Q. (2018). Use of gelatin and gum Arabic for encapsulation of black raspberry anthocyanins by complex coacervation. *International Journal of Biological Macromolecules*, *107*, 1800–1810. https://doi.org/10.1016/j.ijbiomac.2017.10.044
57. Spada, J. C., Marczak, L. D. F., Tessaro, I. C., & Noreña, C. P. Z. (2012). Microencapsulation of β-carotene using native pinhão starch, modified pinhão starch and gelatin by freeze-drying. *International Journal of Food Science and Technology*, *47*(1), 186–194. https://doi.org/10.1111/j.1365-2621.2011.02825.x
58. Šturm, L., Osojnik Črnivec, I. G., Istenič, K., Ota, A., Megušar, P., Slukan, A., Humar, M., Levic, S., Nedović, V., Kopinč, R., Deželak, M., Pereyra Gonzales, A., & Poklar Ulrih, N. (2019). Encapsulation of non-dewaxed propolis by freeze-drying and spray-drying using gum Arabic, maltodextrin and inulin as coating materials. *Food and Bioproducts Processing*, *116*, 196–211. https://doi.org/10.1016/j.fbp.2019.05.008
59. Sukri, N., Multisona, R. R., Zaida, Saputra, R. A., Mahani, & Nurhadi, B. (2021). Effect of maltodextrin and arabic gum ratio on physicochemical characteristic of spray dried propolis microcapsules. *International Journal of Food Engineering*, *17*(2), 159–165. https://doi.org/10.1515/ijfe-2019-0050
60. Tao, Y., Wang, P., Wang, J., Wu, Y., Han, Y., & Zhou, J. (2017). Combining various wall materials for encapsulation of blueberry anthocyanin extracts: Optimization by artificial neural network and genetic algorithm and a comprehensive analysis of anthocyanin powder properties. *Powder Technology*, *311*, 77–87. https://doi.org/10.1016/j.powtec.2017.01.078
61. Tien, N. N. T., Le, N. L., Khoi, T. T., & Richel, A. (2022). Optimization of microwave-ultrasound-assisted extraction (MUAE) of pectin from dragon fruit peels using natural deep eutectic solvents (NADES). *Journal of Food Processing and Preservation*, *46*(1), e16117.
62. Tonon, R. V., Brabet, C., & Hubinger, M. D. (2010). Anthocyanin stability and antioxidant activity of spray-dried açai (Euterpe oleracea Mart.) juice produced with different carrier agents. *Food Research International*, *43*(3), 907–914. https://doi.org/10.1016/j.foodres.2009.12.013
63. Tupuna, D. S., Paese, K., Guterres, S. S., Jablonski, A., Flôres, S. H., & Rios, A. de O. (2018). Encapsulation efficiency and thermal stability of norbixin microencapsulated by spray-drying using different combinations of wall materials. *Industrial Crops and Products*, *111*, 846–855. https://doi.org/10.1016/j.indcrop.2017.12.001
64. Wang, H., Tong, X., Yuan, Y., Peng, X., Zhang, Q., Zhang, S., Xie, C., Zhang, X., Yan, S., Xu, J., Jiang, L., Qi, B., & Li, Y. (2020). Effect of Spray-Drying and Freeze-Drying on the Properties of Soybean Hydrolysates. *Journal of Chemistry*, *2020*. https://doi.org/10.1155/2020/9201457
65. Wang, H. Y., Qian, H., & Yao, W. R. (2011). Melanoidins produced by the Maillard reaction: Structure and biological activity. In *Food Chemistry* (Vol. 128, Issue 3, pp. 573–584). https://doi.org/10.1016/j.foodchem.2011.03.075
66. Wang, W., & Zhou, W. (2012). Characterization of spray-dried soy sauce powders using maltodextrins as carrier. *Journal of Food Engineering*, *109*(3), 399–405. https://doi.org/10.1016/j.jfoodeng.2011.11.012
67. Wang, Y., Lu, Z., Lv, F., & Bie, X. (2009). Study on microencapsulation of curcumin pigments by spray drying. *European Food Research and Technology*, *229*(3), 391–396. https://doi.org/10.1007/s00217-009-1064-6
68. Yamashita, C., Chung, M. M. S., dos Santos, C., Mayer, C. R. M., Moraes, I. C. F., & Branco, I. G. (2017). Microencapsulation of an anthocyanin-rich blackberry (Rubus spp.) by-product extract by freeze-drying. *LWT - Food Science and Technology*, *84*, 256–262. https://doi.org/10.1016/j.lwt.2017.05.063

69. Yang, M., Wei, Y., Ashokkumar, M., Qin, J., Han, N., & Wang, Y. (2020). Effect of ultrasound on binding interaction between emodin and micellar casein and its microencapsulation at various temperatures. *Ultrasonics Sonochemistry*, *62*. https://doi.org/10.1016/j.ultsonch.2019.104861
70. Yazicioglu, B., Sahin, S., & Sumnu, G. (2015). Microencapsulation of wheat germ oil. *Journal of Food Science and Technology*, *52*(6), 3590–3597. https://doi.org/10.1007/s13197-014-1428-1

Figures

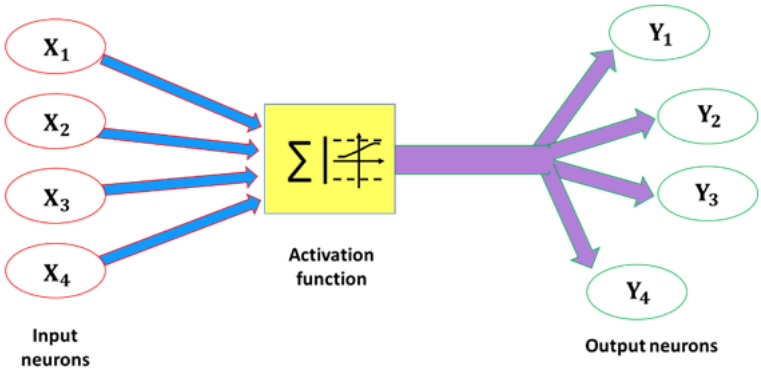

Figure 1

Architecture of proposed feed forward back propagation neural network model.

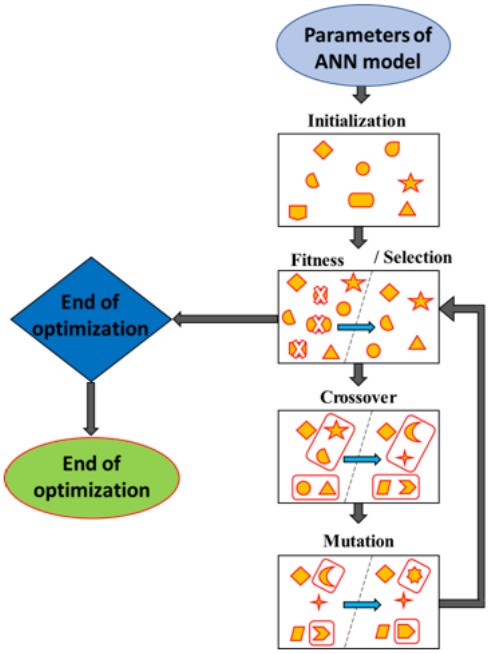

Figure 2

Genetic algorithm for the optimization of freeze-dried encapsulation process.

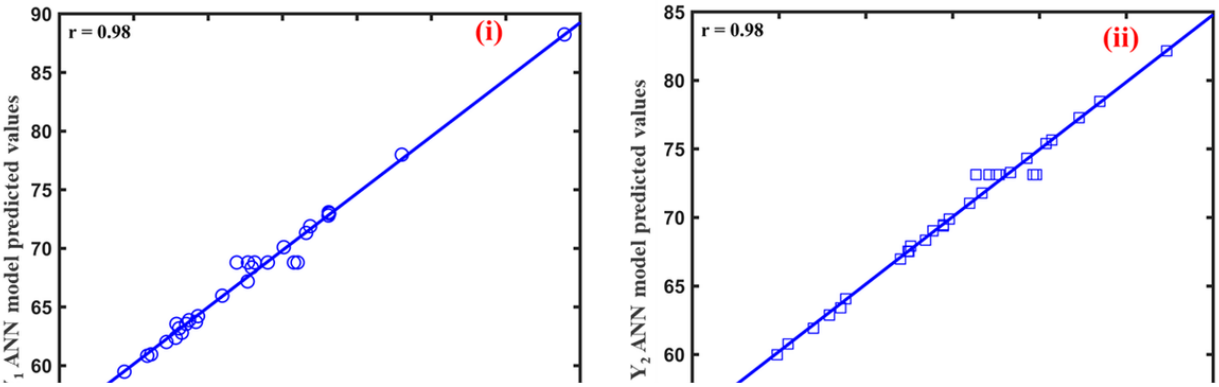

Figure 3

Experimental Vs ANN model predicted values for (i) encapsulation efficiency (Y_1), (ii) antioxidant activity (Y_2), (iii) hygroscopicity (Y_3) and (iv) solubility (Y_4) of freeze-dried encapsulated product of dragon fruit peel extract.

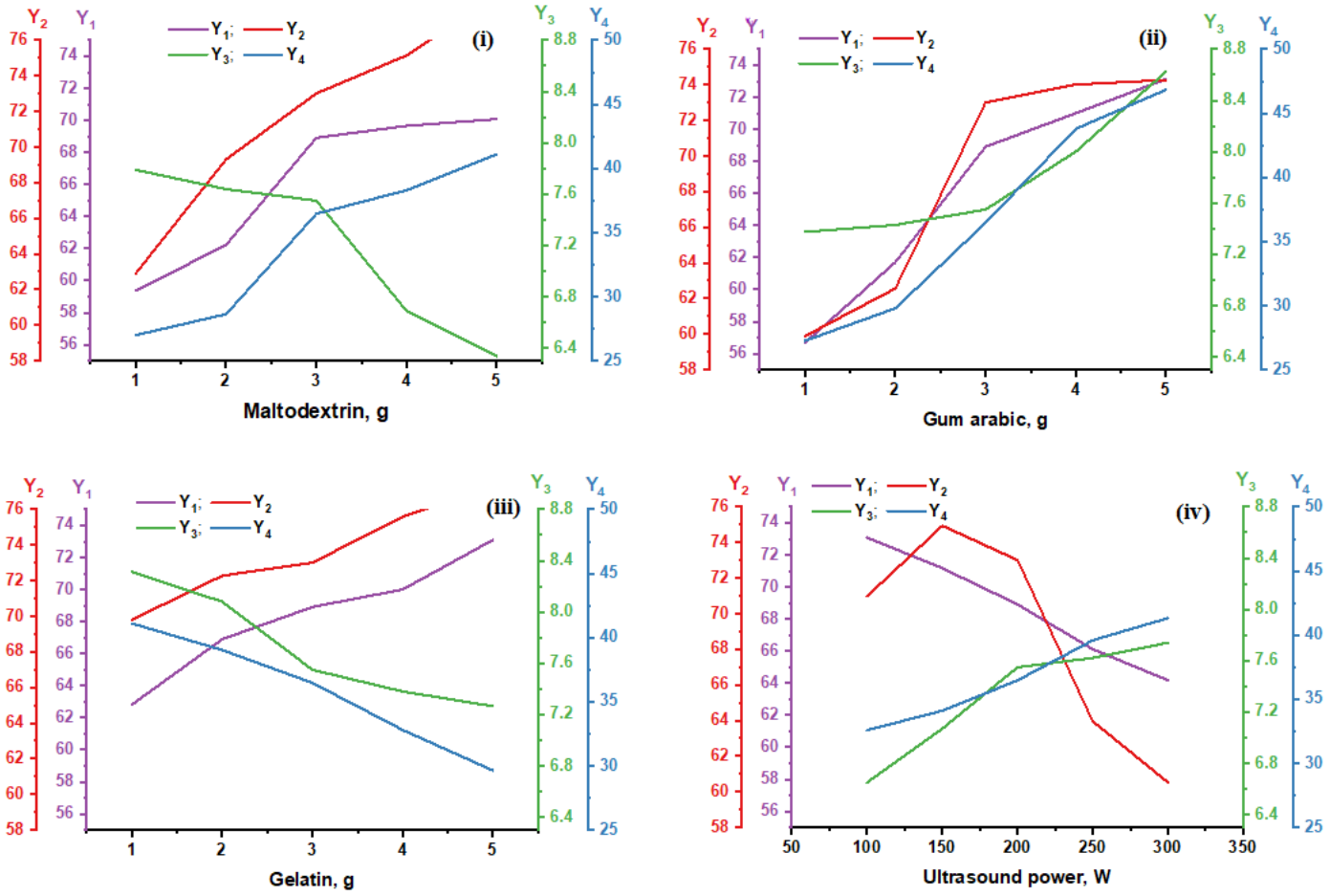

Figure 4

Effect of process parameters (i) maltodextrin, (ii) gumarabic, (iii) gelatinand (iv) ultrasound power on the four responses of freeze-dried encapsulated product of dragon fruit peel extract.

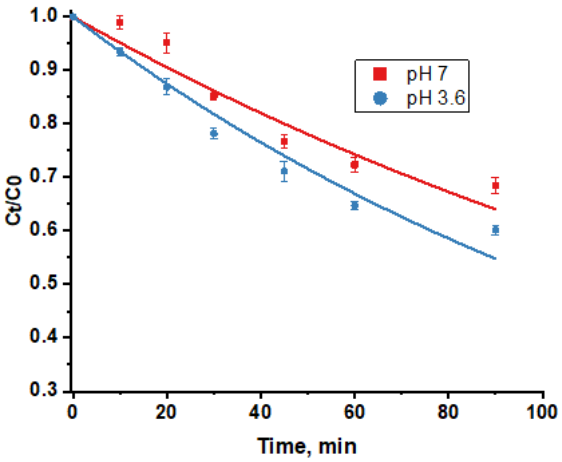

Figure 5

Degradation kinetics of betacyanin in freeze-dried encapsulated product of dragon fruit peel extract at temperature 80 °C and pH of 3.6 and 7.0.

Supplementary Files

This is a list of supplementary files associated with this preprint. Click to download.

- TablesFreezeencapsulationFB.docx
- Graphical.pdf